THE ASTRONOMICAL JOURNAL VOLUME 106, NUMBER 6 DECEMBER 1993

THE 1990 CALÁN/TOLOLO SUPERNOVA SEARCH

MARIO HAMUY

National Optical Astronomy Observatories,[1] Cerro Tololo Inter-American Observatory, Casilla 603, La Serena, Chile
Electronic mail: mhamuy@noao.edu

JOSÉ MAZA

Departamento de Astronomía, Universidad de Chile, Casilla 36-D, Santiago, Chile
Electronic mail: maza@uchcecvm.bitnet

M. M. PHILLIPS AND NICHOLAS B. SUNTZEFF

National Optical Astronomy Observatories, Cerro Tololo Inter-American Observatory, Casilla 603, La Serena, Chile
Electronic mail: mphillips@noao.edu, nsuntzeff@noao.edu

M. WISCHNJEWSKY

Departamento de Astronomía, Universidad de Chile, Casilla 36-D, Santiago, Chile

R. C. SMITH

National Optical Astronomy Observatories, Cerro Tololo Inter-American Observatory, Casilla 603, La Serena, Chile
Electronic mail: rcsmith@noao.edu

R. ANTEZANA

Departamento de Astronomía, Universidad de Chile, Casilla 36-D, Santiago, Chile

L. A. WELLS

National Optical Astronomy Observatories, Cerro Tololo Inter-American Observatory, Casilla 603, La Serena, Chile
Electronic mail: lwells@noao.edu

L. E. GONZÁLEZ

National Optical Astronomy Observatories, Cerro Tololo Inter-American Observatory, Casilla 603, La Serena, Chile and
Departamento de Astronomía, Universidad de Chile, Casilla 36-D, Santiago, Chile
Electronic mail: lgonzalez@noao.edu

P. GIGOUX AND M. NAVARRETE

National Optical Astronomy Observatories, Cerro Tololo Inter-American Observatory, Casilla 603, La Serena, Chile
Electronic mail: pgigoux@naoa.edu, mnavarette@noao.edu

F. BARRIENTOS

Departamento de Astronomía, Universidad de Chile, Casilla 36-D, Santiago, Chile
Electronic mail: barrien@vela.astro.utoronto.ca

R. LAMONTAGNE

Departament de Physique, University of Montreal, Montreal, PQ H3C 3J7, Canada
Electronic mail: lamontag@umtlvr.bitnet

M. DELLA VALLE

La Silla Observatory, European Southern Observatory, Vitacura, Casilla 19001, Santiago, Chile
Electronic mail: mdellava@eso.org

J. E. ELIAS

National Optical Astronomy Observatories, Cerro Tololo Inter-American Observatory, Casilla 603, La Serena, Chile
Electronic mail: jelias@noao.edu

A. C. PHILLIPS

University of Washington, Department of Astronomy, FM-20, Seattle, Washington 98195
Electronic mail: phillips@lick.ucsc.edu

S. C. ODEWAHN

University of Minnesota, Department of Astronomy, 116 Church St. S. E., Minneapolis, Minnesota 55455

 0004-6256/93/106(6)/2392/16/$0.90

J. A. BALDWIN AND A. R. WALKER

National Optical Astronomy Observatories, Cerro Tololo Inter-American Observatory, Casilla 603, La Serena, Chile
Electronic mail: jbaldwin@noao.edu, awalker@noao.edu

T. WILLIAMS

Rutgers University, Department of Physics & Astronomy, P.O. Box 849, Piscataway, New Jersey 08854
Electronic mail: williams@astro.rutgers.edu

C. R. STURCH

Computer Sciences Corporation, Space Telescope Science Institute, Homewood Campus, Baltimore, Maryland 21218

F. K. BAGANOFF

University of California, Department of Astronomy, 405 Hilgard Ave., Los Angeles, California 90025
Electronic mail: baganoff@uclastro.bitnet

B. C. CHABOYER

Yale University, Department of Astronomy, P.O. Box 6666, New Haven, Connecticut 06511
Electronic mail: brian@quednast.bitnet

R. A. SCHOMMER, H. TIRADO, M. HERNÁNDEZ, AND P. UGARTE

National Optical Astronomy Observatories, Cerro Tololo Inter-American Observatory, Casilla 603, La Serena, Chile
Electronic mail: rschommer@noao.edu, htirado@noao.edu, mhernandez@noao.edu, pugarte@noao.edu

P. GUHATHAKURTA

Institute for Advanced Study, School of Natural Sciences, Olden Lane, Princeton, New Jersey 08540
Electronic mail: raja@astrovax.princeton.edu

S. B. HOWELL

Planetary Science Institute, 2421 E. 6th St., Tucson, Arizona 85719
Electronic mail: howell%psikey.span@noao

P. SZKODY

University of Washington, Department of Astronomy, FM-20, Seattle, Washington 98195
Electronic mail: szkody@phast.phys.washington.edu

P. C. SCHMIDTKE

Arizona State University, Department of Physics & Astronomy, Tempe, Arizona 85287-1504
Electronic mail: schmidtke@asucps.bitnet

J. ROTH

California Institute of Technology, 105-24, Pasadena, California 91925
Electronic mail: josh@deimos.caltech.edu

Received 1993 February 3; revised 1993 August 13

ABSTRACT

We have started a search for supernovae as a collaboration between the University of Chile and the Cerro Tololo Inter-American Observatory, with the aim of producing a moderately distant ($0.01 < z < 0.10$) sample of Type Ia and Type II supernovae suitable for cosmological studies. The project began in mid-1990 and continues to the present. This paper reports on the Calán/Tololo discoveries in the course of 1990, and on the spectroscopic and photometric observations gathered for these objects. All of these observations were obtained with CCDs, with the extensive collaboration of visiting astronomers. Great care was exercised in the reduction of the light curves in order to properly correct for the background light of the host galaxy of each supernova. Of the four supernovae found in 1990, one proved to be a SN II-n; the remaining three were members of the Type Ia class at redshifts that ranged between $z=0.04$–0.05. One of the Type Ia events, SN 1990af, was found in the elusive premaximum phase at a redshift of $z=0.0503$, and was observed through maximum light. Peak magnitudes for the other two SNe Ia, which were not observed at maximum light, were derived using a χ^2 minimization technique to fit the data with various template curves that represent a broad range of SNe Ia light curves. In future papers we will make use of these estimates in order to discuss the Hubble diagram of SNe Ia.

1. INTRODUCTION

Given the high intrinsic luminosities of supernovae at maximum light—comparable to the total light of their parent galaxies—astronomers have devoted considerable effort in recent years to investigating the usefulness of these objects as distance indicators. Most attention has been focused on Type Ia supernovae (hereafter referred to as SNe Ia) which have been shown to exhibit an impressive homogeneity in their light curves (Barbon *et al.* 1973; Cadonau *et al.* 1985; Leibundgut 1988) and peak luminosities (Leibundgut & Tammann 1990; Miller & Branch 1990; Branch & Miller 1993). Hamuy *et al.* (1991) found that two SNe Ia that occurred in the same galaxy, SNe 1980N and 1981D in NGC 1316, possessed maximum light magnitudes that differed by less than 0.1 mag, lending considerable support to these claims. However, a recent study by Phillips (1993) of a small sample of well observed SNe Ia suggests that the peak luminosities of these events cover a much greater range than had been before appreciated, and are strongly correlated with the initial decline rate of the *B* light curve.

So far, the study of the Hubble diagram of SNe Ia is based nearly entirely on nearby objects ($z < 0.02$). At such low redshifts, the peculiar motions of individual galaxies introduce a significant scatter in the velocity field associated with the Hubble flow. SNe Ia with larger redshifts scatter more tightly about the relation,

$$\log cz = 0.2m + \log(H_0) - 0.2M - 5, \quad (1)$$

since the peculiar motions of their parent galaxies are much smaller in comparison with their velocities due to the Hubble flow (van den Bergh & Pazder 1992; Tammann & Leibundgut 1990; Leibundgut 1990). In principle, from a well observed sample of such distant SNe Ia, it should be possible to independently estimate the true dispersion in peak luminosity of these objects, and to measure a value for the Hubble constant H_0, *provided the zero point of the absolute magnitude scale of SNe Ia is known.* However, even without a precise knowledge of this zero point, SNe Ia show considerable potential for use in cosmological studies. An example is the recent work by Miller & Branch (1992), who used SNe Ia to examine velocity departures from the Hubble flow. Using the peak apparent magnitudes of SNe Ia, they concluded that the current SN sample was useful to support the existence of the Virgo flow, but was too sparse and local to test large scale flows due to a Great Attractor. This fact led them to conclude that a larger sample of SNe Ia was necessary.

As opposed to SNe Ia, the temporal evolution of Type II supernovae (SNe II), covers a wide range ($\sim$6 mag) of intrinsic brightness over the first 150 days of their evolution, followed by an exponential decay much more uniform in luminosity (Young & Branch 1989; Hamuy & Suntzeff 1990). In spite of the inhomogeneity in the *early-time* light curves of SNe II, these objects also offer considerable potential as distance indicators. Models of the expanding atmosphere of SN 1987A have been used, via a Baade–Wesselink analysis, to measure a distance of 49($\pm$6) kpc to the LMC (Eastman & Kirshner 1989) which is in very good agreement with other distance estimates for this galaxy. This technique has been extended by Schmidt *et al.* (1992) to a number of other relatively nearby SNe II, and could be used to independently measure H_0 from a sample of more distant Type II events.

In mid-1990, a group of staff members of the Cerro Tololo Inter-American Observatory (CTIO) and the University of Chile at Cerro Calán initiated a photographic search for young SNe using the Curtis Schmidt Camera at CTIO. The main goal of this program has been to produce a sample of moderately distant ($0.01 < z < 0.1$) SNe suitable for cosmological studies. This first paper reports on the results of the Calán/Tololo survey obtained in the course of 1990. A general description of the main strategies and techniques employed in the survey is given in Sec. 2.

[1]Cerro Tololo Inter-American Observatory, National Optical Astronomy Observatories, operated by the Association of Universities for Research in Astronomy, Inc., (AURA) under cooperative agreement with the National Science Foundation.

Optical spectroscopy and photometry of the four SNe discovered during 1990 is presented in Sec. 3. Finally, in Sec. 4 we summarize the conclusions of this paper. This survey continues to the present, and forthcoming papers will provide details of the results for 1991 and 1992.

2. THE SURVEY

2.1 The Search

The Calán/Tololo supernova search was begun in 1990 as a continuation of the highly successful search program carried out with the $f/3$ Maksutov Camera (70/100 cm) at the University of Chile's Cerro El Roble Observatory between 1979 and 1984 (Maza *et al.* 1981). In the present survey, we are using the CTIO $f/3.5$ Curtis Schmidt Camera (60/90 cm) which has a 19.05 cm$\times$19.05 cm field and a scale of 96.6 arcsec mm^{-1}, providing a useful sky coverage of 5°$\times$5° when used with photographic plates. Although CCD detectors have recently become available on the Schmidt, the field covered by these (0.5°$\times$0.5°) is not large enough to be competitive with photographic plates in discovering SNe in the redshift range of interest (z=0.01–0.1).

Careful consideration was given to the selection of the most advantageous emulsion for the search. We performed our first tests with 103a-O plates. This emulsion which possesses an effective spectral response that extends from the atmospheric cutoff near 3200 to 5000 Å, was originally chosen since SNe are expected to have a relatively blue color near maximum light. Prior to the observations at the telescope we carried out sensitometry tests for plates baked in Forming gas (98% N; 2% H). We determined that the optimum hypersensitation time was 3 h, providing a gain factor of ~4 (measured at a density of 0.6 above gross fog) with respect to the unbaked plate, and a fog density of 0.3. Subsequent tests on the Schmidt telescope showed that the hypersensitized 103a-O plates yielded a limiting magnitude m_{pg} of ~19 attained with an exposure of 15 min in moonless nights. In hopes of lowering the plate budget, we carried out tests using commercial T-Max 400 film, which is effectively ten times cheaper than plates. Overall, we found that the film has a speed comparable to the 103a-O plates, the main disadvantage being the extremely high number of flaws found on the emulsion. The high number of false SN detections yielded by the film—typically two per field—led us to discard this (cheaper) solution for our program. Beginning in 1991, we tried IIa-O plates which have the same spectral response as the 103a-O plates, but a somewhat lower speed due to the finer grain size of the emulsion. We found that the exposure time required by a IIa-O plate to attain the same deepness as the 103a-O emulsion was 30% higher, i.e., 20 min on the Schmidt Camera. The main advantage of the IIa-O emulsion lies in its improved spatial resolution, which aids significantly in the subsequent visual inspection. To date, we continue using the hypersensitized IIa-O plates which have proved very successful for our project. The optimum baking time in Forming gas for this emulsion has varied between 2 and 4 h, depending on the batch in use.

TABLE 1. Supernova fields observed in 1990.

	α (1950)	δ	Jun	Jul	Aug	Sep	Oct	Nov	Dec
	00 05.0	-37 20	X	X	X	X	X	X	X
*	00 16.0	-49 50		X	X	X	X	X	X
*	00 43.0	-25 30		X	X	X	X	X	X
*	00 58.5	-35 50		X	X	X	X	X	X
	01 16.5	-33 10		X	X	X	X	X	X
	01 29.0	-06 30		X	X	X	X	X	X
*	01 32.0	-29 30		X	X	X	X	X	X
	01 58.0	-55 30		X	X	X	X	X	X
	02 28.8	-08 20		X	X	X	X	X	X
	02 35.5	-00 05		X	X	X	X	X	X
*	02 41.0	-35 10		X	X		X	X	X
	02 52.0	-30 15		X	X	X	X	X	X
	03 09.5	-21 00		X	X		X	X	X
	03 13.5	-39 10		X	X	X	X	X	X
	03 31.0	-20 50		X	X		X	X	X
	03 34.0	-35 00		X	X		X	X	X
	03 34.5	-52 15		X	X		X	X	X
*	03 45.0	-46 25		X	X	X	X	X	X
	04 14.1	-45 29			X		X	X	X
	04 26.3	-57 04		X	X		X	X	X
	04 59.8	-61 19			X	X	X	X	X
*	05 06.3	-35 43			X	X	X	X	X
*	06 15.6	-24 43			X	X	X	X	X
*	07 18.1	-74 45					X	X	X
	07 36.7	-60 56					X	X	X
	09 30.0	+21 10						X	X
	09 51.0	-32 30	X				X	X	X
	10 02.7	-28 00	X				X	X	X
	10 25.8	-34 27	X					X	X
	10 23.0	+19 50						X	X
	10 34.0	-27 12	X					X	X
	10 48.3	+13 41	X						X
	11 17.5	+11 30	X						X
	11 55.5	-28 30	X	X					X
	12 21.5	+11 50	X	X					X
	12 22.0	+16 20	X	X					
	12 42.5	+11 50	X	X					
	12 48.7	-41 00	X	X	X				X
	13 15.0	-24 40	X	X	X				
	13 19.3	-44 40	X	X	X				
	13 27.6	-31 45	X	X	X				
	13 49.3	-30 40	X	X	X				
	19 00.0	-62 30	X	X	X	X	X		
	19 45.0	-57 00	X	X	X	X	X		
*	20 07.4	-49 10	X	X	X	X	X		
*	20 15.5	-44 45	X	X	X	X	X		
*	20 44.5	-71 00	X	X	X	X	X		
	21 07.0	-23 30	X	X	X	X	X		
	21 09.0	-47 00	X	X	X	X	X	X	
	21 25.0	-62 45		X	X		X	X	
*	21 42.0	-53 20		X	X		X	X	
*	21 47.0	-49 30		X	X	X	X	X	
	21 53.5	-33 50		X	X		X	X	
	22 10.5	-44 00	X	X	X	X	X	X	
	22 25.0	-66 30		X	X	X	X	X	
*	22 54.0	-36 00	X	X	X	X	X	X	X
	22 56.0	-39 30		X	X		X	X	X
	23 06.0	-43 30		X	X	X	X	X	X
	23 36.0	-37 15	X	X	X	X	X	X	X
	23 49.0	-30 25		X	X	X	X	X	X

Note: The fields with an asterisk are those that were eliminated as of 1992.

We also seriously considered using a GG-385 filter in our observations. This filter blocks UV light and has the advantage of reproducing the Johnson B band when used with O plates. In principle, this would permit us to measure discovery magnitudes of our SNe in the standard system. However, since SNe are frequently projected on the

TABLE 2. Calán/Tololo supernova discoveries in 1990.

SN Name	Galaxy Name	Galaxy α (1950)	Galaxy δ	Galaxy type	Galaxy z	SN offset ±0.1	SN offset ±0.1	SN m_{pg} ±0.5	SN type	UT discovery date	discoverer
1990S	PGC 38296	12:02:58.6	-29:52:58	S	0.0265	7.6W	5.6N	15.3	II-n	Jul 22.05	Antezana
1990T	PGC 63925	19:54:58.0	-56:23:38	Sa	0.0402	24.8E	1.9S	16.5	Ia	Jul 21.11	Antezana
1990Y	anonymous	03:35:24.2	-33:12:21	E	0.0392	1.0E	5.0S	17.8	Ia	Aug 22.36	Wischnjewsky
1990af	anonymous	21:31:07.7	-62:57:37	E	0.0503	8.0W	7.4N	16.8	Ia	Oct 24.07	Antezana

bright background of their host galaxies, the measurement of precise magnitudes from the photographic plates is a difficult task at best. Since the presence of the filter required a significant increase in the exposure time, we decided to exclude it from our observations.

We spent some time at the beginning of the project deciding on the selection and the number of fields to be included in the program. The original Cerro El Roble project had surveyed sixty fields all located at high Galactic latitudes. We adopted many of the same fields, but with minor modifications of the actual plate centers. With the help of the ESO and Palomar sky surveys, we tuned the position of each field in order to optimize the number of galaxies observed in the $5° \times 5°$ area covered by the Schmidt plates. We decided to replace some fields which did not include a sufficiently large number of galaxies with others that fulfilled this condition. We ended up with the sixty fields which are listed in Table 1 (coordinates correspond to the center of the field), covering from 0 to 24 h in right ascension (the two gaps between 7–9 and 13–19 h correspond to the position of the Galactic disk which hampers our search). These include some well populated areas in the Virgo, Fornax, and Hydra clusters, as well as a few fields in the general direction of the Great Attractor. Given the large area covered by the photographic plates, the resulting sample of galaxies surveyed in our program is not seriously biased toward any particular Hubble type.

In the Cerro El Roble program, a set of 40 plates were taken every month, yielding an average of one supernova discovery per month. At the beginning of the Calán/Tololo program we adopted the same strategy. However, after a few months, we decided to modify this approach with the aim of increasing our chances of discovering the SNe at maximum light, or even before maximum. In particular, we chose to increase the frequency of the observations to two observing runs per month. This led us to decrease the number of fields observed each run to 25, since our plate budget was fixed. As a consequence of this, in the course of 1992 we decreased the total number of fields in the survey to 45. The fields excluded from the survey as of 1992 are those labeled in Table 1 with an asterisk.

The observing procedure on the Schmidt telescope starts by loading the photographic plate in the plate holder, which has been designed to bend the glass according to the curvature of the focal plane of the telescope. For each field we have selected a star of adequate brightness near the center of the frame to be used to guide the Schmidt Camera during the exposure of the plate. The guiding is performed with a CCD detector mounted on a long-focal-length refractor attached to the main body of the telescope. The use of the same guide star from run to run guarantees a perfect registration between plates taken at different epochs. Once the night is over we develop all of the plates in the dark room located on the first floor of the Schmidt telescope building. The development procedure is as follows. First, we start with a 5 min bath of the plate in D-19 developer at 20 C, followed by immersion for 30 s in a stop bath. Next, the plates are fixed for 20 min, and finally washed in running water for 30 min. Once the plates are dry, we send them immediately by bus to Santiago, ~500 km south of CTIO.

The plate scanning is performed by experienced assistants (the same who participated in the Cerro El Roble search) at the Department of Astronomy of the University of Chile. A detailed comparison of each plate with a first epoch exposure is carried out with a Zeiss–Jena blink comparator machine within 24–72 h from the time of observation of the field. Each SN candidate is quickly reported to the CTIO headquarters in La Serena, and a finding chart is sent by FAX to aid identification. Normally, we try to obtain a CCD image with the 0.91 m CTIO telescope in order to confirm the presence of the SN. For reference, around 50% of the candidates found in the course of 1992 (using IIa-O plates) have proved to be real objects. The remaining 50% nearly always correspond to faint images composed of a few grains near the plate limit. These false SNe can be explained in terms of plate defects or statistical variations of the plate background.

2.2 Followup Phase

As soon as we confirm a candidate, photometric monitoring is begun in the $BV(RI)_{KC}$ system (see Bessell 1990 for a recent definition of the passbands) and we attempt to get its spectroscopic classification. It often happens that a spectrograph is not immediately available at CTIO, and so classification cannot be made until a few days afterwards. As a consequence of this, we generally start the photometric monitoring of SNe without the knowledge of the kind of object that we are observing. However, since telescope time is limited, it often becomes necessary to make a selection of the objects that are going to be monitored over a larger period of time. Once we get an idea of the photometric behavior of the SN and its spectroscopic type, we evaluate its usefulness as a distance indicator. For SNe Ia we generally proceed with the photometric monitoring, even if we

TABLE 3. Journal of the observations.

UT DATE	TEL	OBSERVAT	CCD	PHOT/SPEC	OBSERVERS(S)
1990 Jul 25	4.0-m	CTIO	GEC11	SPEC	M. Phillips/J. Baldwin
1990 Jul 25	0.91-m	CTIO	TEK4	PHOT	T. Williams
1990 Jul 26	0.91-m	CTIO	TEK4	PHOT	T. Williams
1990 Jul 26	4.0-m	CTIO	GEC11	SPEC	M. Phillips/J. Baldwin
1990 Jul 26	3.6-m	ESO	...	SPEC	M. Della Valle
1990 Jul 27	0.91-m	CTIO	TI3	PHOT	S. Odewahn
1990 Jul 28	0.91-m	CTIO	TI3	PHOT	S. Odewahn
1990 Jul 29	0.91-m	CTIO	TI3	PHOT	S. Odewahn
1990 Jul 29	4.0-m	CTIO	GEC11	SPEC	A. Walker
1990 Jul 31	0.91-m	CTIO	TI3	PHOT	R. Guhathakurta
1990 Aug 01	0.91-m	CTIO	TI3	PHOT	N. Suntzeff
1990 Aug 12	0.91-m	CTIO	TI3	PHOT	L. Wells
1990 Aug 16	4.0-m	CTIO	GEC11	SPEC	M. Phillips
1990 Aug 21	0.91-m	CTIO	TI3	PHOT	J. Elias
1990 Aug 22	0.91-m	CTIO	TI3	PHOT	J. Elias
1990 Aug 23	0.91-m	CTIO	TI3	PHOT	J. Elias
1990 Aug 24	0.91-m	CTIO	TI3	PHOT	M. Navarrete
1990 Aug 29	0.91-m	CTIO	TI3	PHOT	S. Howell/P. Szkody
1990 Aug 30	0.91-m	CTIO	TI3	PHOT	C. Sturch
1990 Sep 01	0.91-m	CTIO	TI3	PHOT	C. Sturch
1990 Sep 08	0.91-m	CTIO	TI1	PHOT	H. Tirado
1990 Sep 10	1.0-m	LCO	TI1	PHOT	J. Maza/F. Barrientos
1990 Sep 11	1.0-m	LCO	TI1	PHOT	J. Maza/F. Barrientos
1990 Sep 13	1.0-m	LCO	TI1	PHOT	J. Maza/F. Barrientos
1990 Sep 14	1.0-m	LCO	TI1	PHOT	J. Maza/F. Barrientos
1990 Sep 15	0.91-m	CTIO	TI2	PHOT	M. Hernandez
1990 Sep 20	0.91-m	CTIO	TI2	PHOT	J. Roth
1990 Sep 29	0.91-m	CTIO	TI3	PHOT	...
1990 Oct 10	0.91-m	CTIO	TI2	PHOT	N. Suntzeff
1990 Oct 14	4.0-m	CTIO	TEK4	PHOT	M. Navarrete
1990 Oct 20	0.91-m	CTIO	TI3	PHOT	L. Gonzalez
1990 Oct 24	0.91-m	CTIO	TI3	PHOT	L. Gonzalez
1990 Oct 28	0.91-m	CTIO	TI3	PHOT	R. Lamontagne
1990 Oct 28	4.0-m	CTIO	TEK4	SPEC	J. Maza
1990 Oct 28	1.5-m	CTIO	GEC10	SPEC	M. Hamuy
1990 Oct 29	0.91-m	CTIO	TI3	PHOT	R. Lamontagne
1990 Oct 30	0.91-m	CTIO	TI3	PHOT	R. Lamontagne
1990 Oct 31	0.91-m	CTIO	TI3	PHOT	R. Lamontagne
1990 Nov 01	0.91-m	CTIO	TEK4	PHOT	R. Schommer
1990 Nov 02	0.91-m	CTIO	TI2	PHOT	F. Baganoff
1990 Nov 04	0.91-m	CTIO	TI2	PHOT	F. Baganoff
1990 Nov 06	0.91-m	CTIO	TEK4	PHOT	A. Phillips
1990 Nov 08	0.91-m	CTIO	TEK4	PHOT	A. Phillips
1990 Nov 11	1.5 -m	CTIO	TEK4	PHOT	A. Phillips
1990 Nov 13	1.5 -m	CTIO	TEK4	PHOT	A. Walker
1990 Nov 21	0.91-m	CTIO	TI3	PHOT	B. Chaboyer
1990 Nov 22	0.91-m	CTIO	TI3	PHOT	B. Chaboyer
1990 Nov 23	0.91-m	CTIO	TI3	PHOT	M. Navarrete
1990 Dec 14	0.91-m	CTIO	THOM2	PHOT	M. Navarrete
1991 Apr 07	0.91-m	CTIO	TEK2	PHOT	P. Ugarte
1991 Jul 05	0.91-m	CTIO	TI3	PHOT	M. Navarrete
1991 Sep 09	0.91-m	CTIO	TEK2	PHOT	N. Suntzeff
1991 Oct 08	0.91-m	CTIO	TI3	PHOT	N. Suntzeff
1991 Oct 22	0.91-m	CTIO	TEK1	PHOT	M. Hamuy
1991 Oct 23	0.91-m	CTIO	TEK1	PHOT	M. Hamuy
1991 Oct 24	0.91-m	CTIO	TEK1	PHOT	M. Hamuy
1991 Oct 25	0.91-m	CTIO	TEK1	PHOT	M. Hamuy
1991 Oct 26	0.91-m	CTIO	TEK1	PHOT	M. Hamuy
1992 Feb 05	0.91-m	CTIO	TI3	PHOT	P. Schmidtke
1992 Feb 26	0.91-m	CTIO	TEK1	PHOT	N. Suntzeff
1992 Mar 10	0.91-m	CTIO	TEK4	PHOT	M. Hamuy
1992 May 12	4.0-m	CTIO	Reticon	SPEC	M. Phillips

establish that the object has already reached maximum light. This is not ideal, but it is possible afterwards to estimate the peak magnitude of the light curve from the fit of the template curve of SNe Ia to the observed light curve. On the other hand, if the object proves to be a SN II we continue the photometric followup only when we expect to be able to carry out adequate spectroscopic monitoring. The expanding photosphere method for SNe II requires a few spectra obtained over a period of two months in order to estimate a distance to these objects, and this is only practical when the SN is moderately bright at maximum light ($V < 17$).

TABLE 4. Extinction and transformation coefficients to the standard system.

CCD	UT DATE	B		V		R		I	
		k_b	CT	k_v	CT	k_r	CT	k_i	CT
TEK2	1991 Apr 07	0.34	+0.182	0.16	-0.015	0.10	+0.064	0.07	+0.016
TEK2	1991 Apr 26	0.28	+0.148	0.13	-0.065	0.09	+0.040	0.06	-0.013
TEK2	1991 Apr 27	0.27	+0.209	0.15	-0.036	0.10	+0.019	0.08	-0.005
TEK1	1991 Oct 22	0.33	+0.202	0.22	-0.056	0.17	+0.022	0.13	-0.009
TEK1	1991 Oct 26	0.35	+0.227	0.24	-0.029	0.17	+0.090	0.13	+0.016
TEK1	1992 Feb 26	0.33	+0.241	0.21	-0.048	0.17	+0.023	0.12	-0.005
TEK4	1992 Mar 10	0.40	+0.146	0.27	-0.015	0.21	+0.026	0.15	-0.000
	Adopted		+0.200		-0.050		+0.040		0.000
TI3	1990 Oct 28	0.21	+0.040	0.12	-0.056	...	...	...	...
TI3	1990 Oct 29	0.25	+0.038	0.11	-0.053	...	...	...	...
TI3	1990 Oct 30	0.24	+0.034	0.12	-0.055	...	...	...	...
TI3	1990 Oct 31	0.22	+0.020	0.13	-0.064	...	...	...	...
TI3	1991 Jul 05	...	+0.023	...	-0.051	...	+0.033	...	+0.012
TI3	1992 Feb 05	0.31	+0.029	0.20	-0.047	0.17	-0.017	0.11	+0.001
	Adopted		+0.030		-0.050		+0.030		+0.010

Unfortunately, the appearance of a SN is not predictable. As a consequence of this we cannot schedule the followup observations *a priori*, and we generally have to rely on someone else's telescope time. This makes the execution of this project somewhat difficult. However, through the cooperation of many visiting astronomers and CTIO staff, we have been able to obtain good temporal coverage of the light curves of a number of faint SNe. Most of the photometric monitoring is carried out with the CTIO 0.9 m telescope, although we also have obtained some observations with the CTIO 1.5 m and 4.0 m telescopes, and occasionally with the 1 m telescope at Las Campanas Observatory (LCO). Generally speaking, spectroscopic classification of the new SNe has been obtained with CTIO telescopes (the 4 m and 1.5 m). On a few occasions, the SNe have been observed at the European Southern Observatory (ESO) in La Silla. One spectroscopic observation is generally enough to permit the classification of the object, and we usually reserve followup spectroscopy for selected objects, as explained above.

3. RESULTS OF THE SURVEY IN 1990

3.1 The Photographic Search

The observations with the Curtis Schmidt telescope started in 1990 June when we took our first-epoch set of plates. The search itself started effectively in July and was carried out through December on a monthly basis. Each observing run required 3–5 moonless nights to get the complete set of plates of the observable fields, where each field was observed only once. In the June, July, August, September, and October runs we used 103a-O emulsions which had been in stock for several years at CTIO. Because of the lack of glass plates, in the November and December runs we were forced to use T-Max 400 film. During clear and moonless nights it was possible to attain the limiting magnitude permitted by the plates. However, these conditions were not met in all runs and the resulting limiting magnitude of each plate proved to vary between $m_{pg}=17$–19. In Table 1 we list with crosses the observations gathered during 1990.

In the course of 1990, the Calán/Tololo search yielded four SN discoveries, all of them on the 103a-O plates. Unfortunately, the T-Max film employed in the November and December runs yielded such a large number of false detections of possible SNe that the confirmation of our candidates proved completely impractical. Table 2 lists the four discoveries. For the host galaxies we list their PGC names (Paturel *et al.* 1989) whenever available, their equatorial coordinates, approximate morphological type, and redshift. We obtained accurate coordinates for the galaxies from our plates using an Astrorecord Zeiss/Jena XY engine at the Department of Astronomy of the University of Chile, and derived the morphological classifications from inspection of the numerous subsequent CCD images taken at CTIO of the SNe. Note that we classify PGC 63925 here as Sa (from a deep CCD image obtained with the CTIO 4 m telescope), as opposed to a lenticular galaxy as given in the PGC catalogue. The redshifts are based on our own optical spectroscopic observations of the nuclei of the galaxies. Regarding the SNe, Table 2 gives the offsets in arcsecond with respect to the center of the galaxy (accurately measured from CCD images, which supersede our estimates reported in the IAU circulars derived from the photographic plates); the spectroscopic type; an estimated photographic magnitude (m_{pg}) from the discovery plate (with an accuracy of 0.5 mag); the UT date of such plate; and the name of the discoverer. Figure 1 (Plate 109) shows CCD images obtained in V of the four SNe found in the Calán/Tololo search during 1990.

3.2 Followup Observations

We were able to gather a large number of spectroscopic and photometric observations of the four Calán/Tololo discoveries, thanks to the extensive collaboration of many visiting astronomers and CTIO staff members. Table 3 gives a journal of the observations, listing the UT date, the

telescope used, the observatory, the type of CCD employed, a note about the type of data obtained (spectroscopy or photometry), and the name of the observer. The observations were all made with CCD detectors, either in the direct mode or with a spectrograph. The spectroscopic data were obtained with a variety of gratings, filters, and CCDs providing different spectral coverages from 3200 Å to 1 μ. The wavelength calibration was obtained from the observation of a He–Ar lamp taken at the position of the SN. The flux calibration was performed using nightly sensitivity curves determined from the observation of southern flux standards chosen from the lists of Baldwin & Stone (1984) and Hamuy *et al.* (1992).

Light curves for the SNe were measured from a large number of CCD images obtained with different telescopes under all kinds of weather conditions. A variety of Texas Instruments (TI), Tektronix (TEK), and Thomson chips were employed along with filter sets designed to match the $BV(RI)_{KC}$ system. The *BVR* sets are a combination of Schott glasses, cemented, and antireflection coated, as described by Walker (1993), whereas the I filters used are interference filters made by Andover with a typical peak at 8090 Å and a width of 1470 Å. Depending on the telescope/CCD combination, the scale of the images varied between 0.3 and 0.8 arcsec pixel^{-1}. We calculated the SN brightness from each CCD frame differentially with respect to a sequence of field stars on the same frame in order to minimize the effects of atmospheric extinction. Absolute photometry of these comparison stars was later obtained under fully photometric conditions, with transformation coefficients to the Kron–Cousins *BVRI* standard system determined from observations of a number of standard stars, covering a wide range in colors and magnitudes. The standards were taken from the lists published by Landolt (1992) and Graham (1982). We assumed linear transformations to the standard system of the following form,

$$B-b_0=\mathrm{CT}(b-v)+\mathrm{ZP}, \quad (2)$$

$$V-v_0=\mathrm{CT}(b-v)+\mathrm{ZP}, \quad (3)$$

$$R-r_0=\mathrm{CT}(v-r)+\mathrm{ZP}, \quad (4)$$

$$I-i_0=\mathrm{CT}(v-i)+\mathrm{ZP}, \quad (5)$$

where lowercase always refers to instrumental magnitudes measured with an aperture of 14 arcsec in diameter, CT to the color term, and ZP to the zero point of the transformation. The zero subscript refers to magnitudes corrected for the nightly atmospheric extinction which we determined from the measurement of the standards at a wide range of airmasses. Table 4 summarizes the extinction and transformation coefficients determined with different CCDs from the photometric nights.

In order to keep the statistical errors as low as possible, we calculated the instrumental magnitudes of the comparison stars with a small aperture, and then applied the aperture correction necessary to get magnitudes in the same instrumental system employed for the standards. We determined the aperture corrections (which typically varied between 0.04 and 0.08 mag) from the measurement of one or more bright stars on each CCD frame. The large aperture was the same size aperture used for the photometric standards (14 arcsec). We then applied the extinction coefficients and transformation parameters to the instrumental magnitudes in order to derive absolute photometry in the standard system for the sequence of comparison stars.

The measurement of the SN brightness is complicated by the fact that these objects are often projected against the bright background of the host galaxy. To a first approximation, this background can be estimated from an annulus centered around the SN in order to interpolate the galaxy profile at the SN position. However, it is often the case that SNe occur near compact H II regions where this technique would not suffice. Our approach consists of measuring the brightness of the SN for all epochs through an aperture of constant size (in arcseconds). After the SN has faded, we determine the residual background of the galaxy in the aperture used for the SN,[2] and then apply a correction to all the SN magnitudes. To minimize the effect of background light from the host galaxy in these measurements we used as small an aperture as possible, but also big enough to prevent centering errors, possible stellar profile variations within the image, and seeing variations from image to image. Each object required a specific analysis to determine the optimum aperture. In the future we plan to carry out a comparison between the results obtained with this technique and *point spread function* fitting (DAOPHOT) to the SN image.

Once we determined the most appropriate aperture for a given SN, we calculated magnitudes for the comparison stars and the SN, *all through the same aperture.* Atmospheric extinction corrections for these relative measurements were ignored since the net effect of extinction is a simple additive constant in the instrumental magnitudes of all of the stars in the frame. The observed magnitudes were transformed to the standard system using Eqs. (2), (3), (4), and (5). However, since the comparison stars in the SN fields were not sufficient to determine all of the nightly transformation coefficients, we chose to use the mean color terms for each CCD, and to use the comparison stars only to determine the zero point of the transformations. This is a common approach in photoelectric photometry (Harris *et al.* 1981), and should be applicable to CCD photometry since the CT's for a given CCD are a characteristic of the spectral response of the detector/filter combination, which is not expected to vary significantly in time. Indeed, Table 4 shows that the CT's obtained for TI3 remained quite stable over a period of several months; also the CT's obtained with different TEK chips appear quite stable. Since

[2]The location of the SN aperture on frames where the SN is no longer present is determined from a number of nearby field stars (typically 6–10) which are used to derive the geometrical transformation between the working frame and a master image. The master image is a frame containing the reference stars along with the SN. The program computes the spatial transformation required to map the x–y coordinate system of the master image to the coordinate system of the working image. Three parameters are solved for in the geometrical transformation for each axis, namely, the rotation angle, the scale factor, and the shift in the new origin. The residuals of the transformation are typically 0.5 pixels or less.

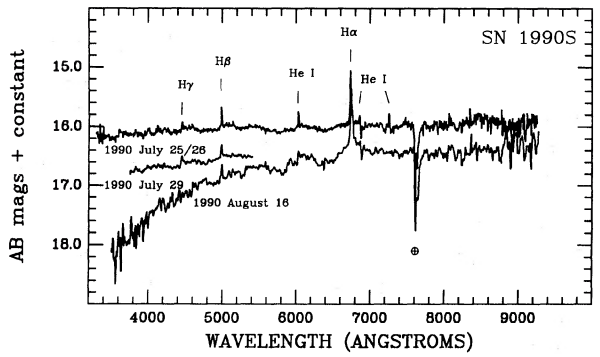

FIG. 2. Spectral evolution of SN 1990S. The spectra are plotted on an AB magnitude scale ($AB = -2.5 \log f_\nu + \text{constant}$), shifted with respect to each other by arbitrary amounts.

the spectral responses of the TEK chips available at CTIO are very similar, we decided to adopt a single set of CT's for this kind of detector. Similarly, for those data obtained with TI1 or TI2, we used the CT's derived from TI3. Note the difference between the CT's in the transformation of the B magnitudes obtained with the TEK chips and TI3. The larger CT yielded by TEK chips is certainly a signature of the sharp drop in sensitivity of this kind of device around 4500 Å.

We were careful to keep track of the errors involved in all of the reduction steps. First, we estimated statistical uncertainties from the number of electrons detected in the SN aperture, and the sky brightness measured in the sky annulus. Errors related to atmospheric extinction were ignored since both the local standard stars and the SN were measured on the same CCD frame. The transformation of the instrumental magnitudes to the standard system yielded a zero point with a typical error ~ 0.02 mag or less, proving always to be much smaller than the statistical uncertainties. Thus, we did not include this error source in the final calculation. Finally, once the background residual in the SN aperture was determined, we added this uncertainty in quadrature to the SN error. Overall, the resulting uncertainties proved to be in the range 0.02–0.03 mag at the beginning of the monitoring, with a steady increase as the object faded. The specific results obtained for each SN are given in the rest of this section.

3.3 SN 1990S

SN 1990S was found by R. Antezana on a plate taken on 1990 July 22.05 (UT) in the spiral galaxy PGC 38296 (ESO 440-G48) at a redshift of $z = 0.0265$ (Hamuy & Maza 1990a). Spectra were obtained on the CTIO 4 m telescope on July 25 and 26, covering the wavelength range from 3200 Å to 1 μ. Figure 2 shows these spectra which reveal a blue continuum along with relatively narrow (~ 800 km s^{-1} FWHM) Hα, Hβ, and Hγ emission lines. Weaker lines of He I $\lambda\lambda$5876, 6678, 7065 are also present in these spectra. The fact that the profiles of the H lines were entirely different than the P Cygni line profiles displayed by the normal members of the SN II class led us to classify

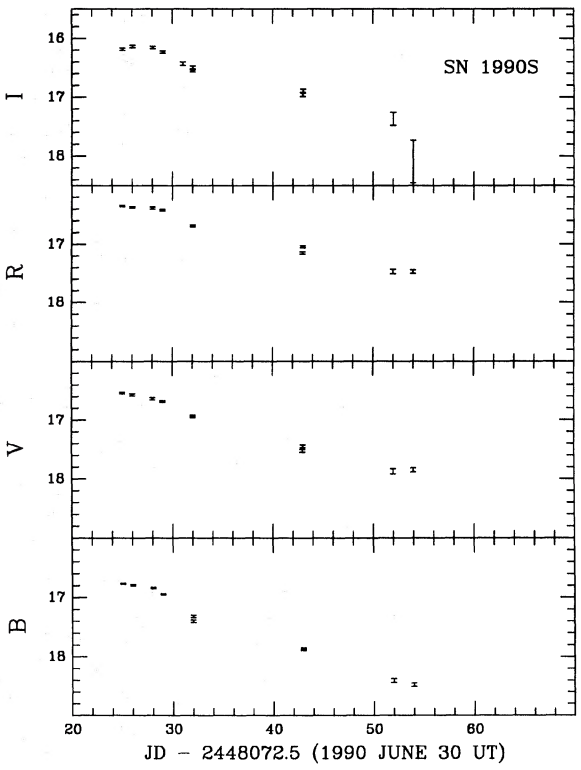

FIG. 3. B, V, R, and I light curves of SN 1990S.

this object as a peculiar narrow subtype (SN II-n) (Schlegel 1990). The spectrum of July 29 showed no significant differences. On August 16, SN 1990S showed some spectral changes, namely a significantly reddening of the continuum, the development of a broad Hα component, and the disappearance of the He lines.

Followup $BV(RI)_{KC}$ photometry of SN 1990S was started on July 25 and continued for a period of one month. Magnitudes for the SN were measured through an aperture of 6.9 arcsec in diameter, with sky taken from an annulus of 4.9 arcsec width at an inner radius of 17.3 arcsec. SN 1990S was embedded in a relatively bright background which yielded the following corrections: 18.270 (± 0.014) in B; 17.618(± 0.024) in V; 17.056(± 0.016) in R; and 16.567(± 0.015) in I. These values were obtained from the observations of the parent galaxy on four different nights once the SN had faded from sight. Figure 3 shows the light curves of SN 1990S after background correction. The SN exhibited a fast decline that lasted for one week after discovery, followed by a slow-decline phase in which the SN declined at a rate of ~ 0.050 mag day^{-1} in B, and somewhat slower in the other bands. This is considerably faster than the decline rate of plateau SNe II. Note that our data showed a maximum in the I light curve around July 27 which was not observed in the other bands. Table 5 lists photometry for the comparison stars selected in the field of SN 1990S (errors are given in brackets in units of mmag, and the number of observations under column heading "n"), which are all identified in Fig. 1 along with SN

TABLE 5. Photometric sequence around SN 1990S.

Star	B-V	V	V-R	R-I	n
1	0.731(018)	17.478(018)	0.431(009)	0.415(013)	4
2	1.455(014)	18.118(011)	0.920(006)	0.874(012)	4
3	0.720(008)	18.743(018)	0.382(013)	0.386(017)	4
4	0.723(005)	17.445(012)	0.412(007)	0.412(007)	4
5	1.349(029)	18.293(015)	0.806(006)	0.697(008)	4
6	0.545(008)	16.801(012)	0.328(009)	0.332(007)	4
7	0.774(008)	16.056(010)	0.473(004)	0.481(011)	4
8	0.833(004)	17.626(007)	0.448(010)	0.440(009)	4

1990S. Table 6 summarizes the photometry that we obtained for SN 1990S (errors are given in brackets in units of mmag) after correction for the underlying galaxy.

3.4 SN 1990T

SN 1990T was found by R. Antezana in the galaxy PGC 63925 (z=0.0402) on a plate taken on 1990 July 21.105 (UT) (Hamuy & Maza 1990b; Phillips & Gouiffes 1990). Figure 1 shows SN 1990T and the host galaxy, revealing that PGC 63925 is an early spiral as opposed to the lenticular classification given in the PGC catalogue (Paturel *et al.* 1989). We obtained spectra of SN 1990T at CTIO and the European Southern Observatory (ESO) at La Silla on July 26, promptly after discovery, and two spectra at CTIO on August 16 covering the wavelength range 4000–9200 Å. Figure 4 shows these observations. The first spectrum revealed the characteristic Si II λ6355 absorption of SNe Ia, with an expansion velocity of 8660 km s^{-1}. Its strength was consistent with a SN Ia about two weeks after B maximum light. The second spectrum showed a weak Si II absorption, as well as some absorptions attributed to Ca II and Fe II, typical of a SN Ia several weeks past maximum.

SN 1990T was monitored photometrically in the $BV(RI)_{KC}$ system for a period of four months. In order to compute a magnitude we used an aperture of 5.3 arcsec in diameter, and a sky annulus 2.2 arcsec in width with an inner radius of 6.7 arcsec. From images of PGC 63925 obtained in the course of 1991 we found that the residual brightness of the galaxy at the SN position was very small, and that further background corrections to the SN magnitudes were unnecessary. Figure 5 shows the light curves of

TABLE 6. Photometry for SN 1990S.

JD − 2448072.5 (June 30)	B	V	R	I
25.03	16.769(009)	16.539(015)	16.347(011)	16.184(020)
26.03	16.793(012)	16.572(018)	16.373(013)	16.137(021)
28.03	16.843(013)	16.640(022)	16.382(019)	16.155(020)
29.03	16.949(011)	16.688(014)	16.418(013)	16.232(018)
31.03	...	...	...	16.432(030)
32.04	17.320(018)	16.947(019)	16.685(017)	16.544(028)
32.04	17.402(021)	16.935(021)	16.688(018)	16.503(032)
43.00	17.880(017)	17.525(025)	17.151(020)	16.955(034)
43.02	17.861(018)	17.448(024)	17.043(019)	16.897(031)
52.00	18.401(032)	17.874(046)	17.473(038)	17.372(110)
54.00	18.475(031)	17.849(034)	17.475(031)	18.094(361)

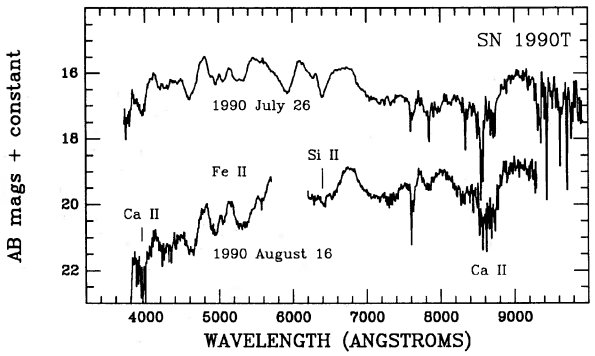

FIG. 4. Spectral evolution of SN 1990T. The spectra are plotted on an AB magnitude scale ($AB=-2.5\log f_\nu+$constant), shifted with respect to each other by arbitrary amounts.

SN 1990T which confirm very clearly that this object was found several days after maximum light. Figure 6 compares the B and V light curves of SN 1990T with three different SN Ia templates, namely, the fast-declining event SN 1986G (Phillips *et al.* 1987), the average curves calculated by Leibundgut (1988), and the slow-decline SN 1991T (Phillips *et al.* 1992). These templates cover a wide range in the morphology of light curves displayed by SNe Ia. Before performing this comparison we modified all of the templates according to the K terms calculated by Hamuy *et al.* (1993) for SNe Ia for a redshift of z=0.04. The templates were also stretched to account for time dilatation

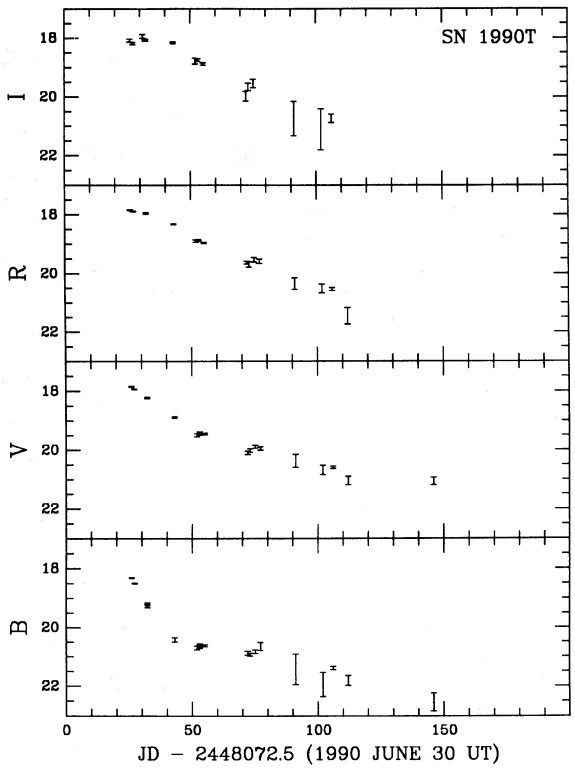

FIG. 5. *B*, *V*, *R*, and *I* light curves of SN 1990T.

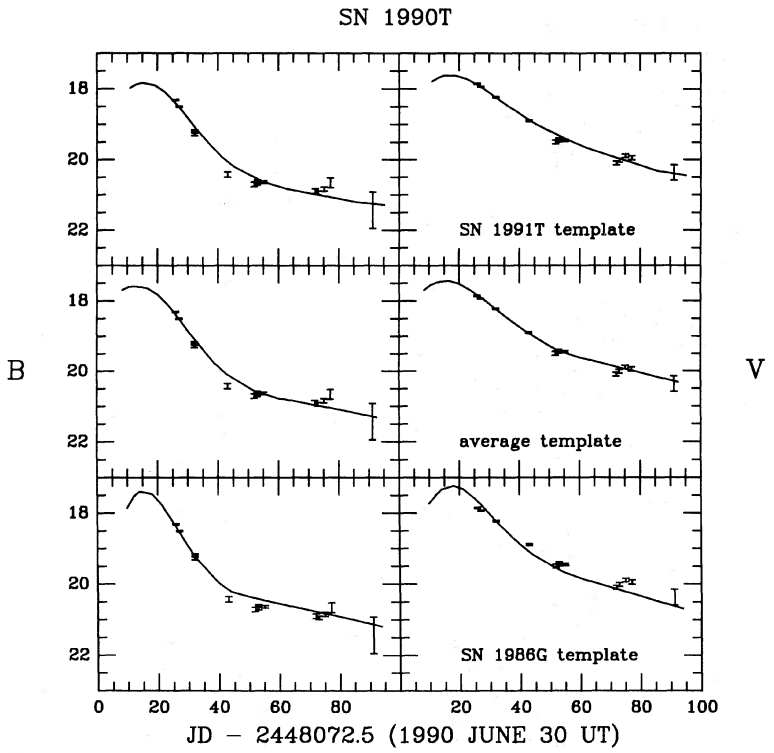

FIG. 6. The *B* and *V* light curves of SN 1990T are compared to the slow-declining SN 1991T template light curves (top panel), to the SNe Ia average templates calculated by Leibundgut (1988) (middle panel), and to the fast-decliner SN 1986G templates (bottom panel). All of the templates were properly modified by the *K*-terms and the time dilatation calculated by Hamuy *et al.* (1993).

(assuming that the Universe is expanding), and then fitted to the observed points. The fits were performed using a χ^2 minimization procedure, solving simultaneously for the time of maximum in *B*, and the peak magnitudes B_{MAX}, and V_{MAX}. In Table 7 we summarize the parameters for the three fits along with 2σ variance uncertainties, and the value of reduced χ^2. It can be seen from the reduced χ^2 values listed in this table that the best representation of the SN 1990T light curves is obtained with Leibundgut's templates, and the worst is obtained with the SN 1986G templates. The goodness of the fits can be visually judged in Fig. 6. All three fits yield similar values for the time of maximum light of around 1990 July 14 UT, in very good agreement with our spectroscopic dating. On the other hand, the peak magnitudes obtained by fitting the different templates show differences which are considerably greater than the errors in each fit. The estimates of B_{MAX} disagree by up to 0.46 mag depending on the template employed. This difference drops to 0.37 mag in V_{MAX} due to the fact that the extrapolation in magnitude from the observed points to the peak of the light curve in this band is smaller. These differences must be taken as upper limits of the uncertainty in the true B_{MAX} and V_{MAX} values of SN 1990T since we have chosen to fit template curves with some of the most extreme SNe Ia subtypes. On the other hand, the 2σ errors quoted in Table 7 for the derived B_{MAX} and V_{MAX} values must be taken as the lower limit to the uncertainty, since we are not fitting models of the light curves, but rather crude templates which have great uncertainties in themselves. These uncertainties have not been taken into account in the fit, except through our attempt to fit the three separate template light curves. Thus, we estimated the true B_{MAX} and V_{MAX} of SN 1990T by taking a straight average of the values given in Table 7, i.e., $B_{MAX}=17.59\pm0.23$ and $V_{MAX}=17.43\pm0.19$.

TABLE 7. Maximum magnitudes for SN 1990T.

TEMPLATE	T^B_{MAX}			B_{MAX}	V_{MAX}	χ^2_{RED}
SN 1991T	1990	July	16.1	17.83	17.62	10.2
			±0.5	±0.05	±0.03	
Leibundgut	1990	July	13.6	17.58	17.43	6.1
			±0.4	±0.04	±0.03	
SN 1986G	1990	July	15.0	17.37	17.25	37.6
			±0.3	±0.04	±0.03	

Note in Fig. 5 that the *I* light curve displayed a secondary maximum around August 1st at $I=18.00$ (±0.05), which is a feature common to other SNe Ia. For example, *I* band observations of the type Ia SN 1991T (Balonek *et al.* 1992) show that the secondary maximum occurred $\sim$23 days after the maximum in *V*, in reasonable agreement with our estimates of the date of B_{MAX} for SN 1990T.

Table 8 lists the photometry for the comparison stars selected in the field of SN 1990T (errors are given in brack-

TABLE 8. Photometric sequence around SN 1990T.

Star	B-V	V	V-R	R-I	n
1	0.540(023)	17.387(013)	0.336(015)	0.327(021)	3
2	1.259(156)	18.566(045)	0.734(051)	0.628(029)	3
3	0.479(017)	18.353(018)	0.335(029)	0.232(051)	3
4	0.623(128)	19.019(045)	0.294(049)	0.294(045)	3
5	0.975(018)	16.374(008)	0.615(008)	0.530(004)	3
6	0.890(005)	14.533(004)	0.482(003)	0.418(005)	3
7	0.983(009)	15.306(003)	0.537(002)	0.471(004)	3
8	0.649(014)	16.678(010)	0.333(009)	0.352(009)	3

ets in units of mmag, and the number of observations under column heading "*n*"). Except for stars 6 and 8, all of the comparison stars are identified in Fig. 1 along with SN 1990T (star 6 is located about 50 arcsec west from star 4; star 8 is located about 90 arcsec north from star 2). Table 9 summarizes the photometry obtained for SN 1990T (errors are given in brackets in units of mmag).

3.5 SN 1990Y

SN 1990Y was found by M. Wischnjewsky in an anonymous elliptical galaxy on a plate taken on 1990 August 22.36 (UT) (Maza *et al.* 1990). This SN was located 1 arcsec east and 5 arcsec south of the center of the parent galaxy, close enough to hamper the followup observations. A spectrum of SN 1990Y obtained on August 29 with the Shane 3 m telescope at Lick Observatory showed that this SN was a member of the Ia subclass (Filippenko & Shields 1990), around one month after maximum light. Della Valle *et al.* (1990) obtained a spectrum of SN 1990Y on August 30 with the 3.54 m New Technology Telescope, which showed the characteristic Si II λ6355 absorption of a SN Ia with an expansion velocity of 9000 km s^{-1}. They also reported absorptions due to Fe II, Na I, and Mg II, and indicated that the SN was 15–20 days past maximum light.

TABLE 9. Photometry for SN 1990T.

JD - 2448072.5 (June 30)	B	V	R	I
26.00	18.316(018)	17.854(015)	17.843(017)	18.082(050)
27.20	18.504(015)	17.939(012)	17.894(014)	18.185(040)
31.20	...	...	...	17.936(062)
32.29	19.277(040)	18.233(020)	17.950(016)	18.062(036)
32.29	19.175(021)	18.220(012)	17.967(011)	18.055(025)
43.17	20.427(074)	18.896(022)	18.329(014)	18.162(028)
52.00	20.704(066)	19.495(054)	18.900(039)	18.777(101)
53.04	20.670(047)	19.458(028)	18.877(021)	18.744(047)
53.04	20.610(042)	19.404(026)	18.875(021)	...
55.17	20.634(036)	19.450(026)	18.956(020)	18.880(039)
72.17	20.892(065)	20.098(057)	19.631(052)	19.976(162)
73.10	20.938(048)	20.018(054)	19.692(087)	19.655(120)
75.00	20.841(058)	19.887(050)	19.534(073)	19.546(142)
77.17	20.659(138)	19.949(060)	19.587(074)	...
91.17	21.438(513)	20.371(223)	20.349(202)	20.743(585)
102.00	21.948(411)	20.678(158)	20.515(149)	21.111(702)
106.08	21.392(055)	20.590(041)	20.540(049)	20.735(149)
112.06	21.808(167)	21.047(147)	21.457(283)	...
146.00	22.540(300)	21.071(128)	...	...

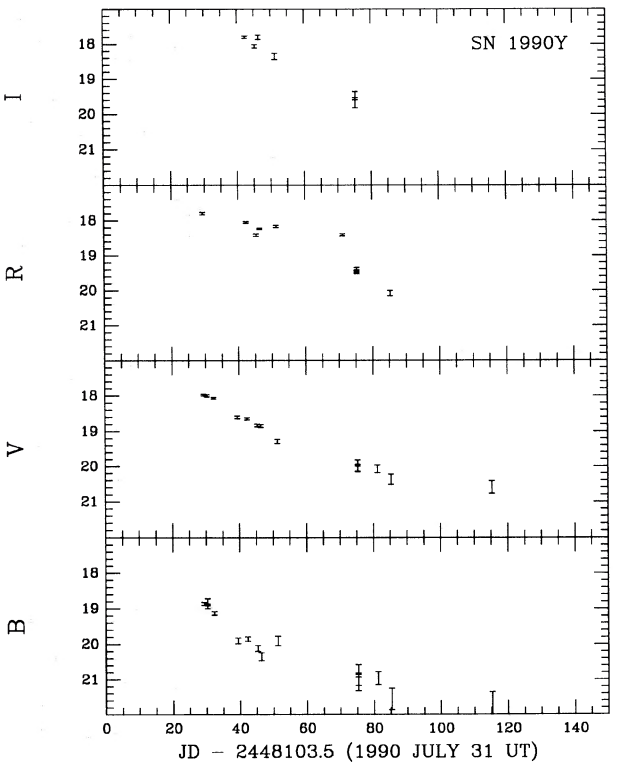

FIG. 7. *B*, *V*, *R*, and *I* light curves of SN 1990Y.

We later obtained an accurate measurement of the redshift of the parent galaxy with the CTIO 4 m telescope, yielding a value of $z=0.0392$.

Promptly after confirmation of SN 1990Y, we initiated $BV(RI)_{KC}$ followup photometry for a period of three months. We chose to use a very small aperture for the calculation of the SN magnitudes in order to keep the contamination of the parent galaxy to a minimum. We adopted an aperture of 4.2 arcsec in diameter, and a sky annulus of 2.6 arcsec in width located at an inner radius of 15.8 arcsec from the object. We estimated the contamination of the host galaxy in the SN aperture from three observations obtained in the course of 1991. We found that the following corrections to the SN magnitudes were necessary: 19.917($\pm$0.064) in *B*; 19.393($\pm$0.054) in *V*; 18.987($\pm$0.022) in *R*; and 18.582($\pm$0.051) in *I*. Figure 7 shows the light curves of SN 1990Y which demonstrates that this object was also found several days after maximum light. In general, the light curves are quite noisy, due mostly to the proximity of the SN to the center of the galaxy which made accurate sky subtraction difficult. Figure 8 compares the *B* and *V* light curves of SN 1990Y with the three different SN Ia templates, properly modified according to the *K* terms calculated by Hamuy *et al.* (1993) for SNe Ia, and stretched to account for the time dilatation. The fits were performed using the same χ^2 minimization procedure described for SN 1990T. In Table 10 we summarize the parameters of the various fits along with 2σ variance uncertainties, and the value of reduced χ^2 for each

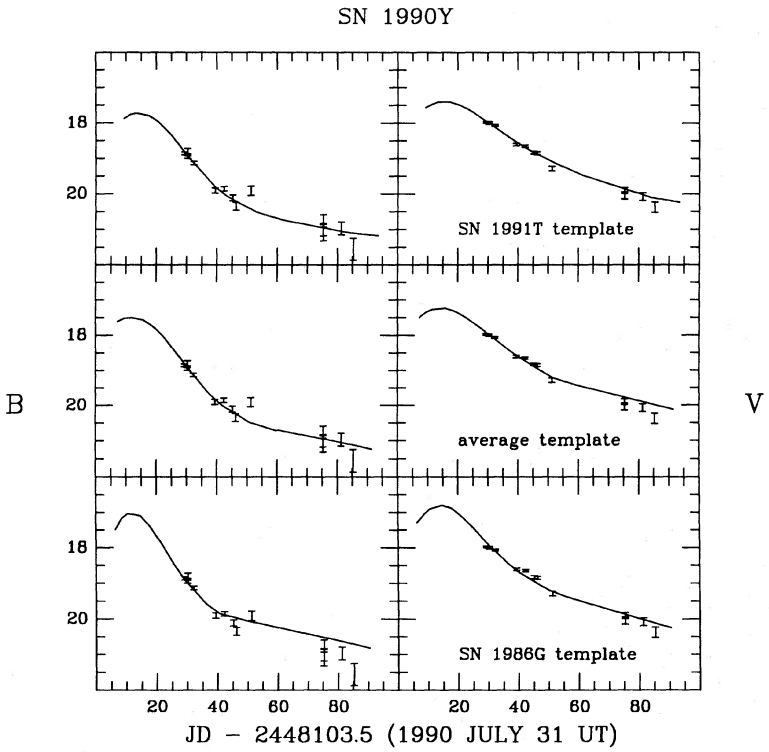

FIG. 8. The *B* and *V* light curves of SN 1990Y are compared to the slow-decliner SN 1991T template light curves (top panel), to the SNe Ia average templates calculated by Leibundgut (1988) (middle panel), and to the fast-decliner SN 1986G templates (bottom panel). All of the templates were properly modified by the *K*-terms and the time dilatation calculated by Hamuy *et al.* (1993).

fit. It can be seen from this table that the best representation of the SN 1990T light curves is obtained with the SN 1991T templates. Leibundgut's average templates also provide a good fit but, the SN 1986G templates yield again a much higher reduced χ^2 value. This can be seen more clearly in Fig. 8. All three fits yield similar values for the time of maximum light, around 1990 August 12 UT, in reasonable agreement with the ESO finding that SN 1990Y was 15–20 days past maximum light on August 30, but somewhat discrepant with the description given by Filippenko and Shields. The various B_{MAX} values disagree by up to 0.72 mag depending on the template employed, and by 0.59 mag in V_{MAX}. In the same manner as for SN 1990T, we provide final estimates of the B_{MAX} and V_{MAX} values for SN 1990Y by taking a straight average of the values given in Table 10, i.e., $B_{MAX}=17.41\pm0.37$, and $V_{MAX}=17.15\pm0.30$.

The data obtained in *R* and *I* in this case were quite sparse. A secondary maximum in the *I* light curve (like that seen in SN 1990T) was not observed since the photometry in this band was not initiated until one month after V_{MAX}.

Table 11 lists the photometry for the comparison stars selected in the field of SN 1990Y (errors are given in brackets in units of mmag, and the number of observations under column heading "*n*"). Except for stars named 8 and 9, all of the comparison stars are identified in Fig. 1 along with SN 1990Y (star 8 is located about 130 arcsec west from star 6; star 9 is located about 120 arcsec east from star

TABLE 10. Maximum magnitudes for SN 1990Y.

TEMPLATE	T^B_{MAX}	B_{MAX}	V_{MAX}	χ^2_{RED}
SN 1991T	1990 August 14.5	17.72	17.40	1.9
	±1.5	±0.14	±0.09	
Leibundgut	1990 August 12.5	17.50	17.23	3.2
	±1.2	±0.11	±0.07	
SN 1986G	1990 August 11.6	17.00	16.81	7.3
	±0.9	±0.08	±0.06	

TABLE 11. Photometric sequence around SN 1990Y.

Star	B-V	V	V-R	R-I	n
1	1.081(020)	17.542(010)	0.545(007)	0.556(012)	2
2	0.875(024)	17.508(017)	0.507(016)	0.444(004)	2
3	1.872(071)	18.684(021)	1.080(047)	1.280(013)	2
4	0.668(043)	17.531(010)	0.397(013)	0.416(016)	2
5	1.459(110)	18.567(007)	0.952(022)	1.082(023)	2
6	0.470(015)	15.148(007)	0.291(005)	0.292(005)	2
7	0.749(023)	16.723(009)	0.431(005)	0.395(006)	2
8	1.308(177)	18.477(012)	0.701(009)	0.689(021)	2
9	0.621(013)	15.905(010)	0.368(008)	0.366(006)	2

TABLE 12. Photometry for SN 1990Y.

JD - 2448103.5 (July 31)	B	V	R	I
29.40	18.865(040)	17.974(022)	17.800(033)	...
30.38	18.792(075)	18.000(030)	...	...
30.38	18.959(040)	17.993(030)	...	...
32.35	19.130(046)	18.065(025)	...	...
39.40	19.906(077)	18.606(037)	...	...
42.31	19.855(064)	18.646(030)	18.050(022)	17.801(033)
45.33	20.117(084)	18.829(041)	18.416(036)	18.056(049)
46.38	20.351(113)	18.849(038)	18.239(020)	17.804(062)
51.35	19.908(130)	19.287(062)	18.170(033)	18.348(091)
71.21	...	...	18.404(026)	...
75.33	21.003(175)	20.050(100)	19.377(033)	...
75.33	21.127(197)	20.044(100)	19.457(035)	19.476(118)
75.33	20.722(136)	19.906(088)	19.485(036)	19.672(142)
81.25	20.970(184)	20.076(110)	...	...
85.31	21.560(309)	20.372(144)	20.081(080)	...
115.31	21.732(373)	20.591(174)	...	...

6). Table 12 summarizes the final photometry obtained for SN 1990Y (errors are given in brackets in units of mmag).

3.6 SN 1990af

SN 1990af was found by R. Antezana in an anonymous elliptical galaxy on a plate taken on 1990 October 24.07 (UT) (Maza & Hamuy 1990). As soon as the candidate was reported to CTIO, a spectrum in the wavelength range 4500–6600 Å was obtained with the 4 m telescope, and another covering from 6500–9000 Å with the 1.5 m telescope. Figure 9 shows the combined spectrum, revealing that SN 1990af was a Type Ia event. The spectrum showed the characteristic Si II λ6355 absorption of SNe Ia, as well as features generally associated with S II and Fe II. The spectrum of the nucleus of the parent galaxy yielded a redshift of $z=0.0503$. The appearance of the SN spectrum and the expansion velocity of 12 040 km s^{-1} derived for the Si II absorption, suggested to us immediately that SN 1990af had been caught before or near maximum light. Therefore, we made a concerted attempt to obtain the best possible observations of the light curves of this object.

Since we were relying on visiting astronomers' telescope time, we decided to limit the observations of SN 1990af to only the *B* and *V* filters. Because of the relative faintness of the supernova, we were able to carry out the monitoring of this object for a period of only one month, down to a *B* magnitude of 21. For the photometry, we adopted an aperture of 5 arcsec in diameter, and a sky annulus of 2.5 arcsec of width located at an inner radius of 6.9 arcsec from the object. We estimated the contamination of the host galaxy in the SN aperture from two observations obtained in the course of 1991. We found that the following corrections to the SN magnitude were necessary: 21.141 ($\pm$0.281) in *B*; and 20.283($\pm$0.045) in *V*. Figure 10 shows the light curves of SN 1990af. Overall these are very well defined, showing that maximum light occurred first in

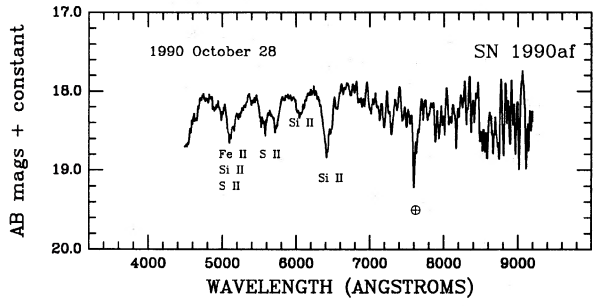

FIG. 9. The spectrum of SN 1990af on 1990 October 28, plotted on an *AB* magnitude scale ($AB=-2.5\log f_\nu+$constant).

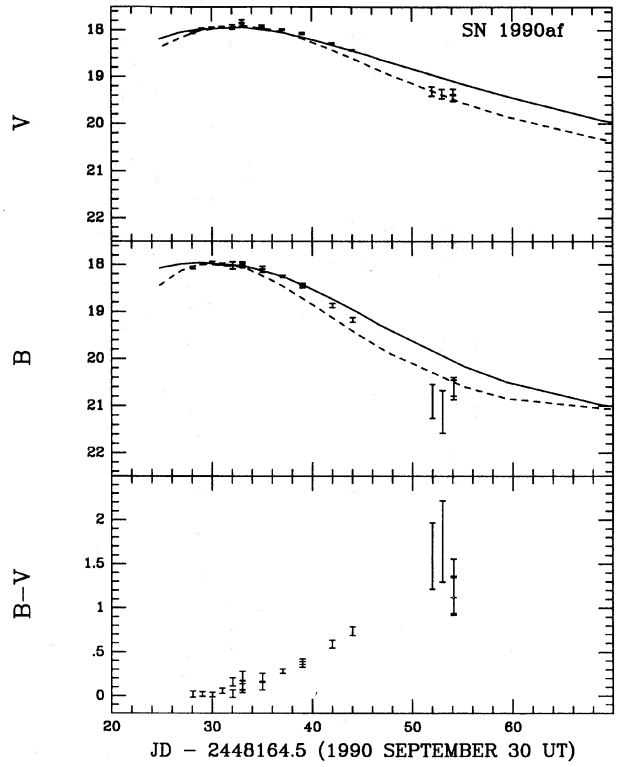

FIG. 10. *B* and *V* light curves and $B-V$ color evolution of SN 1990af. The observations are compared to the SNe Ia average templates calculated by Leibundgut (1988), and to the fast-declining SN 1986G templates, properly modified by the *K*-terms and the time dilatation calculated by Hamuy *et al.* (1993).

TABLE 13. Photometric sequence around SN 1990af.

Star	B-V	V	n
1	0.932(009)	17.433(013)	6
2	0.620(089)	19.654(036)	5
3	0.649(013)	16.362(008)	6
4	0.597(018)	15.672(008)	6
5	0.803(028)	17.829(015)	1
6	0.734(002)	14.635(001)	1
8	0.720(004)	15.605(002)	1
9	1.343(012)	16.546(005)	1
10	0.560(010)	16.640(005)	1
12	1.131(014)	16.147(008)	5
13	1.446(089)	19.169(040)	5
14	1.396(082)	19.036(018)	5

TABLE 14. Photometry for SN 1990af.

JD − 2448164.5 (Sept 30)	B	V
28.10	18.069(026)	18.051(023)
29.04	17.988(021)	17.969(018)
30.03	17.962(022)	17.948(016)
31.03	17.991(023)	17.934(018)
32.07	17.978(035)	17.955(026)
32.07	18.062(039)	17.905(026)
33.04	17.981(037)	17.895(034)
33.04	18.032(042)	17.804(031)
33.04	17.994(040)	17.879(034)
33.04	18.004(041)	17.882(033)
35.04	18.069(033)	17.958(028)
35.04	18.130(038)	17.919(026)
37.07	...	17.995(011)
37.07	18.258(024)	17.977(011)
39.03	18.462(029)	18.073(016)
39.03	18.426(029)	18.067(015)
42.01	18.869(043)	18.279(013)
44.04	19.169(049)	18.431(013)
52.01	20.903(362)	19.312(102)
53.01	21.126(449)	19.370(101)
54.13	20.659(211)	19.321(061)
54.13	20.594(200)	19.460(065)
54.13	20.596(200)	19.444(068)

B, around 1990 October 30 (± 1) UT at $B_{MAX}=17.96$ (± 0.02), and three days later in the visual with $V_{MAX}=17.87$ (± 0.03). Superposed on Fig. 10 we have plotted Leibundgut's (1988) average curves for SNe Ia (solid line) and SN 1986G templates (dashed line), properly modified for the K-terms calculated by Hamuy *et al.* (1993) for $z=0.05$ and for the time dilatation effect. This comparison shows that SN 1990af had a rate of decline after maximum light significantly higher than the average templates and somewhat lower than SN 1986G, but none of the templates provide a satisfactory fit for all epochs. The bottom panel of Fig. 10 shows the $(B-V)$ color evolution of SN 1990af, from $(B-V)\sim 0$ at B maximum to $(B-V)\sim 1.2$ one month later, which resembles the evolution of typical SNe Ia.

Table 13 lists the photometry for the comparison stars selected in the field of SN 1990af (errors are given in brackets in units of mmag, and the number of observations under column heading "n"). Except for stars 5, 10, and 14, all of the comparison stars are identified in Fig. 1 along with SN 1990af (star 5 in located about 30 arcsec north and 50 arcsec east from star 8; star 10 is located about 60 arcsec north from star 6; star 14 is located about 10 arcsec south and 40 arcsec east from star 12). Table 14 summarizes the photometry obtained for SN 1990af (errors are given in brackets in units of mmag).

4. CONCLUSIONS

We have presented the results of the first year of the Calán/Tololo supernova survey. Spectra and light curves were obtained of the four SNe discovered in the course of 1990. One object was found to be a SN II-n; the remaining three were SNe Ia. Of the three SNe Ia found in the course of 1990 in this survey, SN 1990af was discovered before maximum, allowing a precise determination of the maximum light magnitude of this object in B and V. Although SNe 1990T and 1990Y were not caught until ~ 2 weeks after maximum, we have used a χ^2 minimization technique to estimate the maximum light magnitudes. In both cases we find that Leibundgut's average templates of SNe Ia are a good representation of the observed light curves. The slow-decline SN 1991T templates also fit the data reasonably well, but the templates of the fast-decline SN 1986G do not appear to be a good match to the observations. This approach of fitting various templates permitted us to estimate the B and V peak magnitudes of SNe 1990T and 1990Y with an accuracy ~ 0.2–0.3 mag, with this uncertainty being dominated by the lack of independent knowledge of the true light curve shapes.

The Calán/Tololo survey continues to the present. A total of forty SNe have been discovered at redshifts ranging between $z=0.01$–0.1. We have been able to gather followup spectroscopy and photometry for most of these SNe. In future papers we plan to present further results and, in particular, a study of the Hubble diagram of SNe Ia.

This paper has been possible thanks to Grant No. 92/0312 from Fondo Nacional de Ciencias y Tecnología (FONDECYT-Chile). We are deeply indebted to the large number of CTIO visiting astronomers who gathered data for this program. We would also like to thank Marcelo Bass for the photographic work done for this paper.

REFERENCES

Baldwin, J. A., & Stone, R. P. S. 1984, MNRAS, 206, 241
Balonek, T. J., Jameel, M. A., Ford, C. H., Herbst, W., & Ratcliff, S. J. 1992, ApJ (in press)
Barbon, R., Ciatti, F., & Rosino, L. 1973, A&A, 25, 241
Bessell, M. S. 1990, PASP, 102, 1181
Branch, D., & Miller, D. L. 1993, ApJ, 405, L5
Cadonau, R., Sandage, A., & Tammann, G. A. 1985, in Supernovae as Distance Indicators, edited by N. Bartel (Springer, Berlin), p. 151
Della Valle, M., Danziger, J., & Gouiffes, C. 1990, IAU Circ., No. 5083
Eastman, R. G., & Kirshner, R. P. 1989, ApJ, 347, 771
Filippenko, A., & Shields, J. C. 1990, IAU Circ., No. 5083
Graham, J. A. 1982, PASP, 94, 244
Hamuy, M., & Maza, J. 1990a, IAU Circ., No. 5058
Hamuy, M., & Maza, J. 1990b, IAU Circ., No. 5061
Hamuy, M., Phillips, M. M., Maza, J., Wischnjewsky, M., Uomoto, A., Landolt, A. U., & Khatwani, R. 1991, AJ, 102, 208
Hamuy, M., Phillips, M. M., Wells, L. A., & Maza, J. 1993, PASP, 105, 787
Hamuy, M., & Suntzeff, N. B. 1990, AJ, 99, 1146
Hamuy, M., Walker, A. R., Suntzeff, N. B., Gigoux, P., Heathcote, S. R., & Phillips, M. M. 1992, PASP, 104, 533
Harris, W. E., Fitzgerald, H. P., & Reed, B. C. 1981, PASP, 93, 507
Landolt, A. U. 1992, AJ, 104, 340
Leibundgut, B. 1988, Ph.D. thesis, University of Basel

Leibundgut, B. 1990, in Supernovae, edited by S. E. Woosley (Springer, Berlin), p. 751
Leibundgut, B., & Tammann, G. A. 1990, A&A, 230, 81
Maza, J., & Hamuy, M. 1990, IAU Circ., No. 5124
Maza, J., Phillips, M. M., & Suntzeff, N. B. 1990, IAU Circ., No. 5080
Maza, J., Wischnjewsky, M., Torres, C., González, L., Costa, E., & Wroblewski, H. 1981, PASP, 93, 239
Miller, D. L., & Branch, D. 1990, AJ, 100, 530
Miller, D. L., & Branch, D. 1992, AJ, 103, 379
Paturel, G., Fouqué, P., Botinelli, L., & Gougenhein, L. 1989, Catalogue of Principal Galaxies (Observatories de Lyon et Paris-Meudon)
Phillips, M. M. 1993, ApJ, 413, L105
Phillips, M. M., *et al.* 1987, PASP, 99, 592
Phillips, M. M., & Gouiffes, C. 1990, IAU Circ., No. 5066
Phillips, M. M., Wells, L. A., Suntzeff, N. B., Hamuy, M., Leibundgut, B., Kirshner, R. P., & Foltz, C. B. 1992, AJ, 103, 1632
Schlegel, E. M. 1990, MNRAS, 244, 269
Schmidt, B. P., Kirshner, R. P., & Eastman, R. G. 1992, ApJ, 395, 366
Tammann, G. A., & Leibundgut, B. 1990, A&A, 236, 9
van den Bergh, S., & Pazder, J. 1992, ApJ, 390, 34
Walker, A. R. 1993, in Stellar Photometry-Current Techniques and Future Developments, IAU Colloquium No. 136, Dublin, edited by Ian Elliot (in press)
Young, T. R., & Branch, D. 1989, ApJ, 342, L79

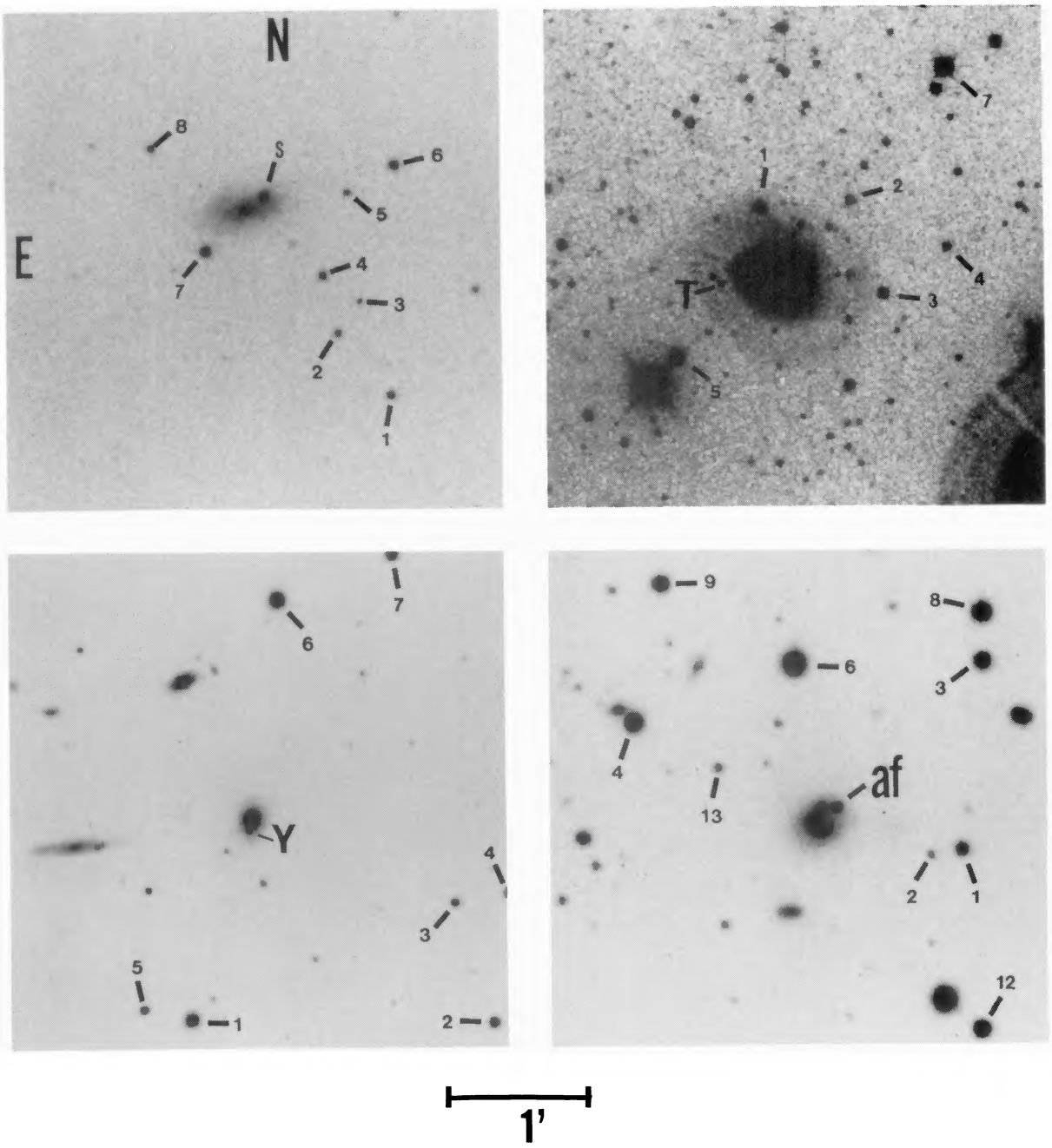

FIG. 1. Direct images of SNe 1990S, 1990T, 1990Y, and 1990af obtained with a *V* filter with different CCDs. The stars of the photometric sequences are also labeled along with the SNe.

Hamuy *et al.* (see page 2398)